Modelling EMG Driven Wrist Movements using a Bio-inspired Neural Network

Yinfeng Fang, Jiani Yang

School of Communication Engineering, Hangzhou Dianzi University, Hangzhou 310018, China.

Dalin Zhou, Zhaojie Ju

Intelligent Systems and Biomedical Robotics Group, School of Computing, University of Portsmouth, Portsmouth PO1 3HE, U.K.

Abstract

The hidden pattern within the sEMG signal has wide applications in human-robot interaction. Decoding the patterns from sEMG signal tends to use black box models, which limits the further analysis of the mechanism of human musculoskeletal system. Therefore, a bio-inspired neural network (BNN) is proposed to model the information propagation procedures from nerve-related information (i.e. EMG signal) to muscle activation to joint activation to extremity movements. Instead of random parameter initialisation, the priori knowledge, such as muscle-electrode relationship, and muscles' functionality, are fully considered to initialise the parameters. Besides, an interpretability constraint error back propagation algorithm (ICBP) is proposed to fine-tune the model for movement prediction, without scarifying model's interpretability. An open sEMG database ISRMyo-I is utilised to verify the proposed methods for the classification of six wrist movements. With the only input of mean absolute value (MAV) feature, the proposed approach achieves an accuracy of >82%, which outperforms the support vector machine (78%), linear discriminant analysis (80%), k-nearest neighbors (78%), multi-layer perceptron (69%), random forest (74%), and convolutional neural network (74%).

Keywords: Musculoskeletal Modelling, Bio-inspired Neural Network, Wrist Motion Recognition

1. Introduction

Surface electromyography (sEMG) signal is the sum of the potentials of all motor units around the electrodes on skin surface [1]. It can be acknowledged that, the generation of a series of hand gestures is a very complicated process. According to electrophysiology knowledge, first of all, the human brain produces contraction consciousness and emits a series of nerve impulses. Immediately, the electrical impulses are transmitted to corresponding muscles, stimulating a certain number of motor units to participate in contraction activities. Eventually, muscle fibers drive joints to generate corresponding hand gestures. During the process of action generation, sEMG signals are the weak electrical signal that directly related to the nerve activities [2]. Therefore, sEMG signals have a significant embodiment of the expansion and contraction strength of finger joints. In recent years, with the increasing requirement of human-machine interface (HMI) and the rapid development of computer technology, sEMG is widely used in prostheses [3, 4, 5], the control of skeleton or robots [6], rehabilitation training [7,8], signal language recognition [9], and sports exercises [10], and etc.

Decoding hand gesture or muscle contraction force from sEMG signal becomes a popular research topic recent years. Taking sEMG features as input, machine learning technology is widely applied, including SVM [11], LDA [12], neural network [13], Gaussian mixture model [14], granular models [15], and etc. Recent years, deep learning approaches, including convolutional neural networks (CNN) or recurrent neural networks (RNN), are widely applied in sEMG based hand motion recognition [16,17]. Zhang et al. [18] utilise RNN to decode 21 hand gestures from raw EMG signals, and reach the accuracy of about 89.6%for the classification. Chen et al. [19] utilise a CNN to extract sEMG features and then feed to SVM and LDA for hand motion classification, and find that combining CNNFeat with traditional features can improve the accuracy by

4.35%, 3.62% and 4.7% for SVM, LDA and KNN, respectively. Although deep learning approaches can achieve higher accuracy in the comparison with other classifiers and raw sEMG signals can be directly used without feature extraction [18,19], these approaches are of low interpretability as discussed in [20,21].

Generally, the mentioned machine learning frameworks map input signal to prediction results, in which the parameters are difficult to be linked with the physiological knowledge of human motions, such as muscle synergy, and motor unit etc. This issue is concerned by several research groups. Jiang et al. [22] highlight that it is invaluable to take the advantage of underlying neurophysiological processes of natural movements for the development of a more natural prosthesis. They explicitly express the sEMG signal as a function of multidimensional neural control information, and a degree-of-freedom-wise (DOF-wise) nonnegative matrix factorization algorithm is proposed to extract the neural control information from the sEMG to provide simultaneous and proportional control signals for multiple DOFs. Piazza et al. [4] take the neuroscientific theories (i.e. postural synergies) in the design and control of a soft bionic hand, demonstrating higher performance. Recently, a neuromorphic model with the input of sEMG signal for the control of prosthetic hand is proposed [23], in which human-like reflex is mimicked, and they believe that mimicking reflex on a prosthetic hand may improve grasping performance and safety when interacting with human. Besides, Xi et al. [24] propose a cortical–muscular functional network using EEG and EMG to explore the motion control mechanism from an explainable point of view.

Feature extraction is also an important utility for improving the performance of classification, which helps to reduce the randomness of the signal as well as to remove some unpredictable noises. It is crucial to explaining EMG feature from a physiological point of view, which can enhance model's interpretability. For instance, the feature of mean absolute value (MAV) is supposed to be related to the muscle contraction force [25], and the feature of median frequency can reflect the fatigue of muscles [26]. Farina et al. [27] use a blind source separation method to extract the timings of activation of each motor unit as EMG feature

from the high density sEMG signal. Li et al. [28] propose a sEMG feature from multiple sEMG channels, called active muscle regions (AMR), which reflects the active muscles while performing hand gestures. Great effort on the research of features and classifiers have witnessed its progress of sEMG based hand gesture recognition, but the stability is still a problem, especially when facing to the interference, like electrode shift [29].

In the era of deep learning and big data, interpretable models with explainable parameters and internal outputs attract great attention [20,21]. A bio-inspired neural network (BNN) is proposed in this paper for decoding multiple channels of sEMG signals to wrist movements, in which muscle group activation (MGA), muscle activation (MA) [30], and muscle-skeloton activation (MSA) are modelled in a layer-by-layer manner. MGA is evaluated by the strength of the captured sEMG signal from an electrode and all the related muscles that would contribute signals to the electrode, belong to one muscle group. MA indicates the degree of contraction of a specific single muscle. MSA is used to evaluate the applied force on the joint.

In addition, all the parameters are initialised according to musculoskeletal knowledge, and a specially designed optimisation algorithm is proposed to maintain parameters' interpretability during the optimisation procedure. To some extends, the proposed model provides a utility to help people understand the reasons of decision-making, explaining the completeness of prediction results [31] The interpretablity of the proposed BNN can be demonstrated in three aspects. 1) The model structure is interpretable. A 3-layer NN is compatible with the principle of human movements, in which nerve activity induces the muscle to contract, and then muscle contraction drives skeleton joints to move; 2) The weights are interpretable. Some weights indicate how a muscle contributes to the signal amplitude of one channel, and some weights indicate how a muscle drives a joint to move. 3) The output of each layer is interpretable. The output of MA layer and MS layer indicate the intensity of muscle activation, and muscle-skeleton activation, respectively.

The remaining of this paper is organized as follows. Section 2 presents the

BNN model, including parameter initialisation and optimisation approaches. Section 3 and 4 illustrate the experimental setup and the results with discussions, respectively. Section 5 concludes this study with future works.

2. Methods and Materials

2.1. Neural Network Modelling for sEMG to Action Propagation

In order to solve the problem of low transparency and poor interpretability in the decoding process by traditional approaches, this paper proposes an interpretable BNN model containing three layers, including MGA layer, MA layer, and MS layer, as seen in Figure 1. The input of the network is the MGA ($e = [e_1, \cdots, e_{n_0}]$) and the output is the skeleton joint state ($y = [y_1, \cdots, y_{n_2}]$); the output of the MGA is the single muscle activation ($s = [m_1, \cdots, m_{n_1}]$), where n_0 is the nubmer of sEMG channels); n_1 is the number of muscles involved in the movements; n_2 is the number of DoFs. Muscle group refers to muscle combination in which all muscles contributes electric activities to the captured sEMG signal from an electrode. e_i is closely related to the raw sEMG signal. The signals from one sEMG channel reflex the activation of the muscles under the corresponding electrode. This paper takes MAV as the muscle group activation, since MAV is almost linearly to the muscle force [32], and has been widely accepted as the sEMG feature for hand gesture recognition [33,34]. The skeleton joint state (y_i) is the angle of each DoF, such as the angle of wrist that determines wrist flexion and extension. Besides, the output of the MA layer is the activation of each muscle (m_i).

2.2. Physiology Driven Weights Initialization

Parameter initialisation is an elemental step for neural network optimisation. For a general neural network, random parameter initiation using normal or uniform distribution is always taken. In the proposed model, anatomy and musculoskeletal knowledge are utilised to initialise the parameters. The physical distances between sEMG electrodes and each muscles are taken to initialise

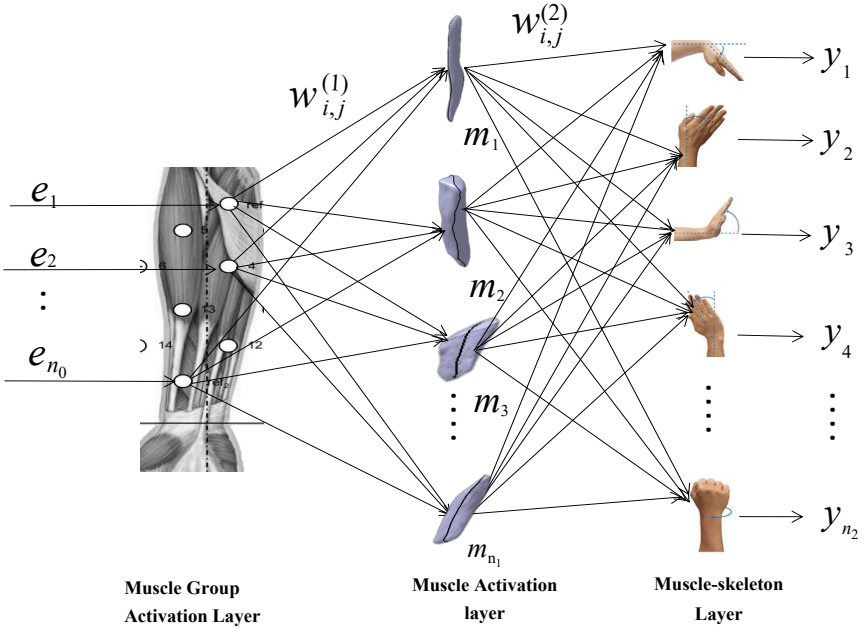

Figure 1: The demonstration of neural network modeling for EMG to upper extremity movement propagation.

$w_{(i,j)}^{(1)}$, and muscle's functionality in anatomy is utilised to initialise the $w_{(i,j)}^{(2)}$. $w_{(i,j)}^{(1)}$ and $w_{(i,j)}^{(2)}$ are the weights between two layers, as demonstrated in Figure 1

2.2.1. $w_{(i,j)}^{(1)}$ initialisation using Electrode-muscle Distance

Suppose that the contribution of a piece of muscle to the sEMG signal captured by an electrode is inversely proportional to the distance between the electrode and the muscle, and then the weight $w_{(i,j)}^{(1)}$ can be deduced from the distance. If each muscle can be physically modelled in a 3D space, and the position of the electrode is fixed, then the distance can be calculated by Equ. 1

$$d_{(i,j)} = \iiint_{\Omega_j} \sqrt{(x - x_0^i)^2 + (y - y_0^i)^2 + (z - z_0^i)^2} dV, \tag{1}$$

where Ω_j is the space occupied by the muscle j, and (x_0^i, y_0^i, z_0^i) is the position of the electrode i. Define the smallest distance as $min(d_{(i,j)})$, and the largest one as $max(d_{(i,j)})$, and then the initial value of $w_{(i,j)}^{(1)}$ can be defined as

$$\hat{w}_{(i,j)}^{(1)} = \alpha \cdot \bar{d}_{(i,j)} - \frac{1}{2}\alpha, \tag{2}$$

where

$$\bar{d}_{(i,j)} = \frac{max(d_{(i,j)}) - d_{(i,j)}}{|max(d_{(i,j)}) - min(d_{(i,j)})|}, \tag{3}$$

and α is a coefficient, which is used to adjust the optimisation performance.

2.2.2. $w_{(i,j)}^{(2)}$ initialisation using musculoskeletal knowledge

In anatomy, nine skeletal muscles control the three DoFs of the hand wrist. The nine skeletal muscles are pronation muscle (M_1), flexor radial wrist (M_2), palmaris longus (M_3), ulnar wrist flexor (M_4), pronation anterior muscle (M_5), extensor carpi radialis longus (M_6), radial extensor carpi brevis (M_7), extensor carpi ulnaris (M_8), and supinator (M_9). Therefore, the number of nodes in the MA layers is set to nine, noted from M_1 to M_9 accordingly. The three DoFs of the wrist involve the movements of pronation/supination(PRO/SUP), flexion/extension(FLE/EXT), and radial/ulnar deviation (RD/UD). This study initialises $w_{(i,j)}^{(2)}$ according to the following formula,

$$\hat{w}_{(i,j)}^{(2)} = \begin{cases} \frac{1}{k_i \sum_{s=1}^{n_j} \frac{1}{k_i}} & \text{if PRO, FLE, or RD} \\ -\frac{1}{k_i \sum_{s=1}^{n_j} \frac{1}{k_i}} & \text{if SUP, EXT, or UD} \end{cases}, \tag{4}$$

satisfying

$$|\sum_{i=1}^{n_j} \hat{w}_{(i,j)}^{(2)}| = 1, \tag{5}$$

where k_i is the number functions of the related muscle i, and n_j is the number of muscles that can be involved in the movement j. To initialize the weights from the MA layer to MS layer, the muscles' functionality in anatomy is studied as follows. M_1 pronates the forearm (PRO) and flexes elbow; M_2 acts to flex (FLE) and abduct the hand (RD); M_3 flexes the wrist (FLE); M_4 controls flexion of

the wrist (FLE) and deviation of the ulnar (UD); M_5 pronates forearm (PRO); M_6 controls extension (EXT) and deviation of the wrist (RD); M_7 controls extension (EXT) and deviation of the wrist (RD); M_8 serves to extend (EXT) and adduct (UD) the hand at the wrist; M_9 supinates the forearm (SUP).

2.3. Interpretability Constraint Error Back Propagation Algorithm

Although the network parameters are initialised by electrode to muscle distance and musculoskeletal knowledge, the electrode position on the forearm skin is only roughly estimated, and the muscle anatomy can be slightly different among subjects. Therefore, an interpretability constraint error back propagation algorithm (ICBP) is proposed. It is an effective algorithm that fine-tunes the parameters without sacrificing model's interpretability. ICBP constrains the searching range for optimization procedure, and thus could avoid possible local optimums.

The MGA layer is the input layer in the network, and this study takes the sigmoid function as the transfer function of the MA layer, formulated as

$$m_j = sigmoid(\sum_{i=1}^{n_0} w_{(i,j)}^{(1)} e_i), \tag{6}$$

where m_j is the j^{th} muscle activation, and e_i is the muscle group activation that is the MAV of a sEMG signal. The transfer function of the MS layer is defined as

$$y_j = tanh(\sum_{i=1}^{n_1} w_{(i,j)}^{(2)} m_i), \tag{7}$$

where y_j is output of the network that implies the hand joint state of the wrist.

For parameter optimisation, this study defines the loss as follows,

$$E = \frac{1}{n_2} \sum_{j=1}^{n_2} \frac{1}{2} (d_j - y_j)^2, \tag{8}$$

where E is the loss; d_j is the expected output; n_2 is the number of output.

$w_{i,j}^{(2)}$ can be updated according to the following formula,

$$w_{i,j}^{(2)}(t+1) = \begin{cases} w_{i,j}^{(2)}(t) - \eta \Delta w_{i,j}^{(2)}(t) & \text{if Case 1} \\ w_{i,j}^{(2)}(t) & \text{if Not Case 1} \end{cases}, \tag{9}$$

where η is the step factor, and

$$\Delta w_{i,j}^{(2)}(t) = -(d_j - y_j)(1 - y_j^2)o_j. \tag{10}$$

In Equ.9, Case 1 is defined as $|w_{i,j}^{(2)}(t+1) - \hat{w}_{(i,j)}^{(2)}| < \delta_1$, which ensures that the optimisation does not influence the interpretability of the parameters.

$w_{i,j}^{(1)}$ can be updated according to the following formula,

$$w_{i,j}^{(1)}(t+1) = \begin{cases} w_{i,j}^{(1)}(t) - \eta \Delta w_{i,j}^{(1)}(t) & \text{if Case 1} \\ w_{i,j}^{(1)}(t) & \text{if Not Case 1} \end{cases}, \tag{11}$$

where η is the step factor, and

$$\Delta w_{i,j}^{(1)}(t) = -\sum_{j=1}^{n_2}(d_j - y_j)(1 - y_j^2)w_{i,j}^{(2)}o_j(1 - o_j)e_i. \tag{12}$$

In Equ.11, Case 1 is defined as $|w_{i,j}^{(1)}(t+1) - \hat{w}_{(i,j)}^{(1)}| < \delta_2$ for interpretability purpose.

3. Experimental Verification

3.1. Experimental Setup and Data Processing

To verify the performance of BNN model for hand gesture recognition, sEMG signals were collected following the rules of the Declaration of Helsinki of 1975, revised in 2008, approved by the ethics Committee of university of Portsmouth (TECH2018-D.Z-02). Figure 2 shows the experimental scenario during data capturing, where subjects were required to follow the hints displayed on the screen to perform hand gestures. The system consists of sixteen bi-polar sEMG channels. For each sEMG channel, the spectrum components beyond the frequency range of 20-500Hz and the 50 Hz power line noise are depressed by two Sallen-Key filters and a notch filter, respectively. The resolution and sampling frequency of the analog-to-digit convertor are set to 12 bits and 1k Hz, respectively. The digitalised sEMG signal is transmitted to a personal computer via USB cable for signal recording and processing. The captured sEMG signals are

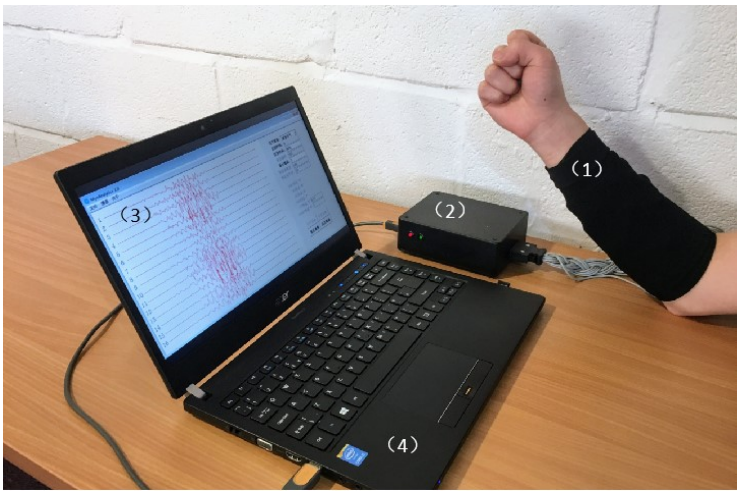

Figure 2: The experimental setup for sEMG signal capturing, including (1) electrode sleeve, (2) sEMG device, (3) sEMG capturing software, and (4) personal computer.

from six subjects, twenty sessions for each subject, two sessions a day (taken in the morning and afternoon respectively), and one trial for each gesture in a session. Although 13 hand gestures were collected, only six wrist movements (wrist flexion (WF), wrist extension (WE), wrist pronation (WP), wrist supination (WS), ulnar flexion (UF) and radial flexion (RF)) were selected to verify the usability of the proposed methods. The captured database has been published 35, and is available the link [1]

To initialise the parameters of $w^{(1)}$, the distances between electrodes and muscles need to be calculated, which requires the 3D information of each muscle on the forearm as well as the electrode position related to these muscles. The extended Cardiac-Torso (XCAT) realistic computer simulation for human muscle system (by Duke University Medical Center, UK) is utilised in this study, which provides the complex anatomy of all muscles of the right forearm. The muscle structure of the forearm and the electrode position related to muscles are demonstrated in Figure 3. The 3D information of muscles are initially processed

[1] https://github.com/yinfengfang/ISRMyo-I.git

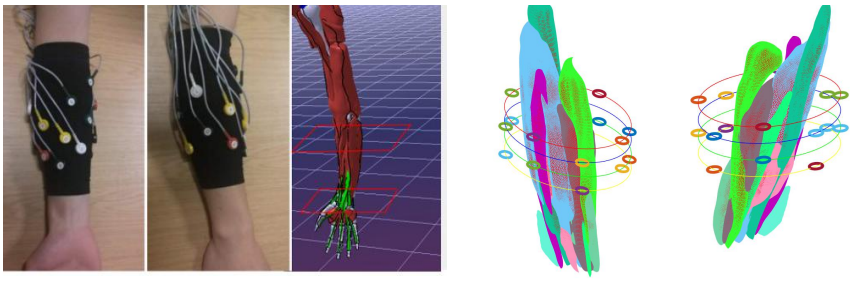

Figure 3: (a) the actual sleeve worn on the right forearm. (b) the 3D virtual muscles of XCAT demonstrated in CATIA software (Dassault Systèmes, France). (c) the simulation of electrodes and muscle position in 3D space, which simulates a schematic diagram of the sleeve with 16 electrodes evenly surrounding the forearm muscles.

in Catia V7 (Dassault Systems ltd., France), and then load to Matlab R2020a (The MathWorks Inc., USA) for numerical calculations. Also, the algorithm of BNN model are implementated in Matlab R2020a. The sEMG signals of the first five seconds of each gesture were excluded to ensure that the samples were correctly labelled, regardless subjects' delayed response to the hints. The overlapped windowing strategy was adopted to segment the sEMG signal stream with 256 ms window length and 64 ms increment. The MAV feature is used as the input for the BNN, as well as the single feature for other pattern recognition approaches for comparison. The total dimension of feature vectors was 16, indicating 16 sEMG channels. The total number of samples after processing is 72000 (12000 samples per subject, 1200 samples per day). After initialisation, BNN will be trained by ICBP algorithm using 600 samples from one session, and then tested by another 600 samples from another session. Both training and testing sessions are from one day of one subject.

3.2. Comparison

This study applies BNN model in hand motion recognition, and compares it with other widely used classifiers. The selected classifiers include SVM with Radial Basis Function (RBF) kernel (rbf-SVM), LDA, kNN, MLP, DT, and

CNN. LDA is typically used as benchmark classifier in this research field and has been commercially applied 36. SVM tends to obtain higher classification accuracy than LDA in a number of studies 36. Decision tree could attain higher accuracy than kNN and SVM in certain experimental scenario 37. MLP is the most similar classier as the proposed BNN. In the experiment, MLP is set to contain two hidden layers with nine and three nodes, respectively. CNN is very popular for

EMG based hand gesture recognition in recent years 18, 19, but it normally requires raw sEMG signal or multiple hand-crafted features to form a matrix as the input. In the current study, samples with the size of 16×1 are transferred to 4×4 matrix as the input for CNN. The constructed CNN contains 5 layers, including input layer, two convolutional layers, a fully connected layer, and an output layer in order.

The classification accuracy is reported in intra-day test scenario where training data and testing data are from the same day. The accuracy is reported as the average one across ten days for each subject.

4. Experimental Results and Discussion

4.1. Weights Initialisation Using Biological Knowledge

For the initialisation of weights connecting MGA layer and MA layer (i.e. $w_{i,j}^{(1)}$), the electrode to muscle distances are calculated according to the Equ. 1 firstly. Table 1 lists the calculated distances, in which M_1 to M_9 indicates the nine muscles and E_1 to E_{16} corresponds to sixteen electrodes. The least distances for each electrode are marked in bold. For instance, the least distance between E_1 and M_5 indicates that the pronator quadratus contributes more to the collected sEMG signal from electrode E_1. In contrast, flexor carpi radial (M_2) contributes least sEMG signal to electrode E_1 due to the largest value. To facilitate the network optimisation procedure, all the distances are normalised in the range between -10 and 10 to initialise the weights of $w_{i,j}^{(1)}$.

Table 2 demonstrates the initialised weight $\hat{w}_{(i,j)}^{(2)}$ between MA layer and MS layer, where rnd means that these weights are randomly initialised by small

Table 1: The Muscle Electrode Distance Calculated in Simulation Environment

Distance		Muscle								
		M_1	M_2	M_3	M_4	M_5	M_6	M_7	M_8	M_9
Electrode	E_1	275	283	201	212	**155**	170	236	246	252
	E_2	264	**167**	184	193	208	274	285	274	282
	E_3	199	211	**154**	169	235	245	251	262	166
	E_4	**182**	193	208	273	284	262	271	188	200
	E_5	**144**	159	224	235	240	251	155	173	183
	E_6	198	262	273	259	268	185	197	**140**	156
	E_7	221	231	236	248	**152**	170	180	195	259
	E_8	270	242	254	171	188	**132**	154	208	222
	E_9	222	237	**145**	168	172	192	245	259	242
	E_{10}	254	171	188	**132**	154	208	222	222	237
	E_{11}	**145**	168	172	192	245	259	236	249	165
	E_{12}	183	**128**	150	202	217	216	232	140	164
	E_{13}	168	188	239	254	245	260	175	195	**146**
	E_{14}	170	217	233	226	244	**156**	181	186	208
	E_{15}	251	268	245	260	175	195	**146**	170	217
	E_{16}	233	226	244	**156**	181	186	208	251	268

values less than 0.1, indicating weak relation between muscles' functionality and the movements.

As can be found in Table 2, $\hat{w}^{(2)}_{(1,1)}$ and $\hat{w}^{(2)}_{(5,1)}$ are positively set, which indicates that muscle M_1 and M_5 are positively related to the movement of PRO in anatomy. Besides, $\hat{w}^{(2)}_{(1,1)}$ and $\hat{w}^{(2)}_{(5,1)}$ are set to 1/3 and 2/3 respectively, because the number of functionality for M_1 and M_5 are 2 and 1, respectively. Additionally, setting $\hat{w}^{(2)}_{(9,2)}$ to -1 can be explained as that M_9 is the only muscle related to motion SUP. Similarly, Table 2 also shows that M_2, M_6 and M_7 equally contribute to motion UD, and M_6, M_7 and M_8 equally contribute to motion

Table 2: The initialisation of $w^{(2)}_{(i,j)}$ according to muscle functionality.

$\hat{w}^{(2)}_{(i,j)}$		Wrist Movements (j)		
		PRO/SUP	RD/UD	FLE/EXT
Muscles (i)	M_1	**1/3**	rnd	rnd
	M_2	rnd	**1/3**	1/4
	M_3	rnd	rnd	**1/2**
	M_4	rnd	**-1**	1/4
	M_5	**2/3**	rnd	rnd
	M_6	rnd	**1/3**	**-1/3**
	M_7	rnd	**1/3**	**-1/3**
	M_8	rnd	rnd	**-1/3**
	M_9	**-1**	rnd	rnd

Note that rnd indicates random small value.

4.2. Weight Fine-tuning Analysis

Figure 4 demonstrates the change of training loss along with the number of iteration under two initialisation strategies, where the utilised data is from the first day of subject one. One curve shows random parameter initialisation result, and the other three are under physiology driven initialisation strategy. The initial loss are 1.06 for physiology driven initialisation, and the other are 1.11, 1.11, and 1.28 for random initialisation. It can be found from Figure 4 that all curves show fast declines before 2000 iterations, and physiology initialisation obtains a more significant loss drop than others, decreasing from 1.06 to about 0.54. Besides, it is also found that physiology initialisation strategy can obtain a more smooth decreasing trend than others. After 20000 iterations, the training loss drops to lower than 0.5 for physiology initialisation, and drops to higher than 0.7 for other three random ones. This experimental result demonstrates that the proposed physiology initialisation strategy would obtain an lower initial loss and final training loss, indicating that the prior knowledge of musculoskeleton and anatomy are worthy of attention for the decoding of hand movement from sEMG signal.

The change of $w^{(1)}_{1,j}$ and $w^{(2)}_{2,j}$ during the fine-tuning process are demonstrated in Figure 5 and Figure 6, respectively, where the utilised data is from the first

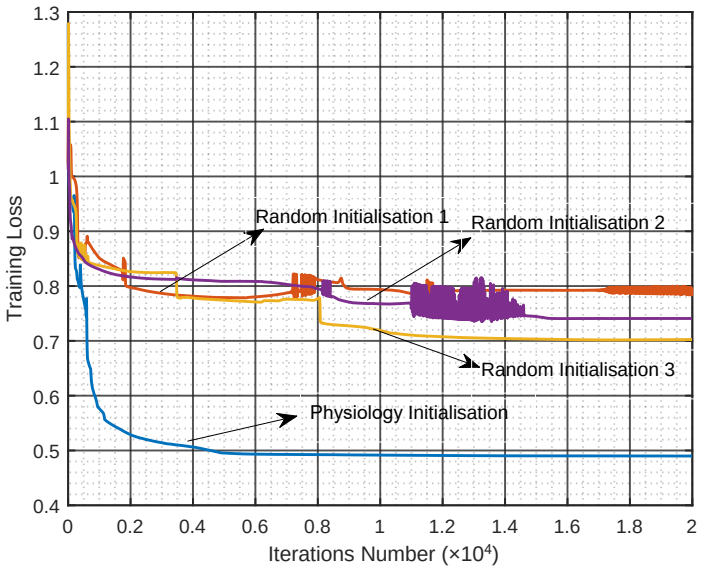

Figure 4: A comparison of the change of training loss along with iterations between random parameter initialisation and physiology driven initialisation.

day of subject one. It can be found in Figure 5 that all the investigated weights change in a small range. The difference between initial value and final value is less than 2, which maintains the fine-tuned weights in an explainable range. The weights of $w_{2,2}^{(2)}$ and $w_{2,3}^{(2)}$ are initialised to 0.33 and 0.25, respectively, according to musculoskeletal knowledge, and $w_{2,1}^{(2)}$ is set to about -0.06 randomly. After 80 iterations, $w_{2,2}^{(2)}$ and $w_{2,3}^{(2)}$ are fine-tuned to 0.47 and 0.10, reaching the top and bottom threshold limited by the ICBP algorithm. Similarly, $w_{2,1}^{(2)}$ is optimised to about -0.22. If traditional BP algorithms was applied for optimisation, these weights might be significantly adjusted and would loss its interpretability.

4.3. Accuracy Comparison with other Classifiers

This study also compares the proposed BNN model with other traditional approaches (SVM, LDA, kNN, MLP, RF, and CNN) in wrist movement classification. The experimental results for six subjects are demonstrated in Table 3. With the normalized MAV feature as input, the BNN model achieves the aver-

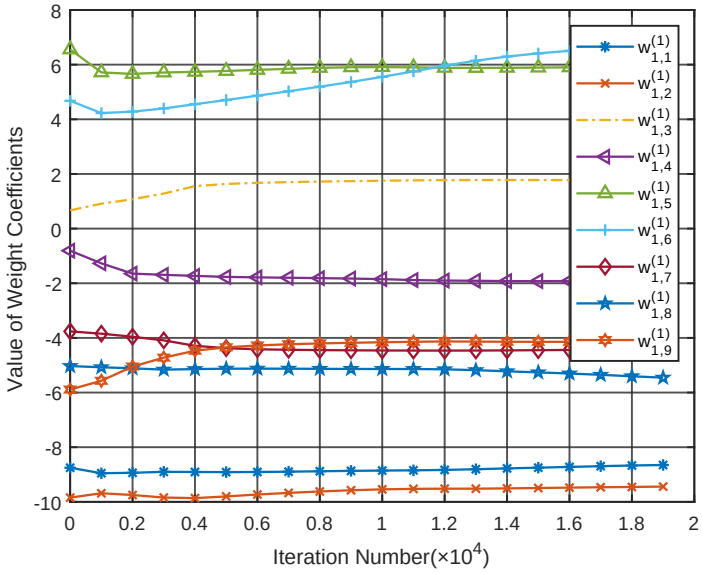

Figure 5: The change of $w_{1,j}^{(1)}$ along with the number of iteration.

aged accuracy at 81.82%, while the other classifiers obtain the average accuracy at 77.58%, 80.81%, 77.89%, 68.94%, 74.39%, and 74.04%, respectively. It is not surprised that the plausible CNN only reaches the accuracy of 74.04%, which is possibly because that the size of input for the used CNN is only 4×4 MAV feature map, which is much smaller than normal images. Besides, the number of training data for CNN in the current study may be not enough to train the CNN sufficiently.

In addition, this study also takes the joint activation as the input for wrist movement classification by traditional classifiers. The investigated classifiers obtain the average accuracies of 82.41% (SVM), 82.15% (LDA), 82.56% (KNN), 76.29% (MLP), and 77.27% (RF), as shown in Table.4. In comparison with using MAV feature as input, the accuracy is improved by about 4% (SVM), 2% (LDA), 5% (KNN), 7% (MLP), and 3% (RF). This result implies that the BNN model can be used to extract biological features from sEMG signals, and these features can enhance movement classification performance.

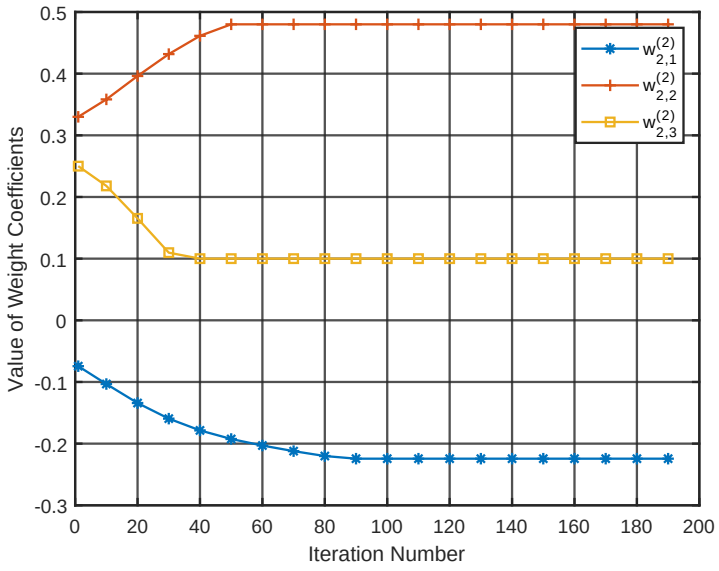

Figure 6: The change of $w_{2,j}^{(2)}$ along with the number of iteration.

4.4. Interpretability Analysis

Figure 7 visualises the joint activation for six wrist movements, where y_1, y_2, y_3 are the axes of joint activation strength for RD/UD, FLE/EXT and PRO/SUP, respectively. As can be found from the figure, these samples for different motions can be clearly separated. In detail, samples of PRO and SUP are clustered around (0.2, 0.01, -0.7) and (0.2, 0.01, 0.65); samples of RD and UD are clustered around (-0.65, 0.1, -0.1) and (0.5, -0.1, 0.1), and samples of FLE and EXT are clustered around (0.1, -0.65, 0.1) and (-0.35, 0.65, 0.09). It is clear that the central points of each motion can be biologically explained by the three dimensional activation. This result also shows that the original 1×16 MAV feature can be dimensional reduced to 1×3 joint activation feature. Although the dimension is reduced, the classification accuracy can be improved as compared between Table 3 and Table 4

Figure 8 demonstrates the muscle activation after optimisation, the strength of which is averaged across six subjects. For the motion PRO, muscle M_5 is most activated, which is consistent with the functionality of M_5. For SUP, muscle

Table 3: Wrist movement classification accuracy(%) comparison with traditional classifiers, where MAV feature is used as the only input for all the algorithms.

Subject	Ours	SVM(rbf)	LDA	KNN	MLP	RF	CNN
A	72.82	72.68	69.35	68.67	64.03	68.90	60.08
B	64.62	58.42	69.52	63.05	57.35	62.25	65.47
C	86.43	85.35	84.83	86.62	71.88	76.40	77.30
D	89.87	88.38	88.73	85.50	80.53	84.25	87.73
E	84.47	78.92	82.47	78.35	61.35	75.95	68.82
F	92.72	81.73	89.37	85.18	78.52	78.60	84.88
Mean	81.82	77.58	80.71	77.89	68.94	74.39	74.04

Table 4: Wrist movement classification accuracy (%) by traditional classifiers with joint activation (i.e. the output of MS layer) as the input.

Subject	SVM(rbf)	LDA	KNN	MLP	RF
A	73.63	72.62	73.92	64.58	69.18
B	68.98	70.20	66.87	60.62	66.47
C	86.25	85.30	87.72	80.73	77.32
D	90.08	92.12	89.95	84.72	84.85
E	82.80	81.12	83.42	80.90	79.40
F	92.73	91.57	93.52	86.22	86.42
Mean	82.41	82.15	82.56	76.29	77.27

M_9 is most activated, and it is right for supinating the forearm. For RD, muscle M_2 is most activated, followed by M_7 and M_6, which is consistent with these muscles' functionality. For UD, M_4, M_7 and M_8 are mostly activated, in which muscle M_4 and M_8 determines the deviation of the ulnar. For the motion of FLE, most of muscles are activated, except M_8 and M_9, which may be because that subjects tend to activate all the muscles when conducting wrist flexion. For the motion of EXT, the muscles of M_1, M_4 and M_6 are mostly activated. These muscles involve the motion PRO, FLE/UD and EXT/RD, which maybe because subjects conduct EXT along with PRO, UD, or RD. In sum, the extracted single muscle activation are closely related to the corresponding wrist movements,

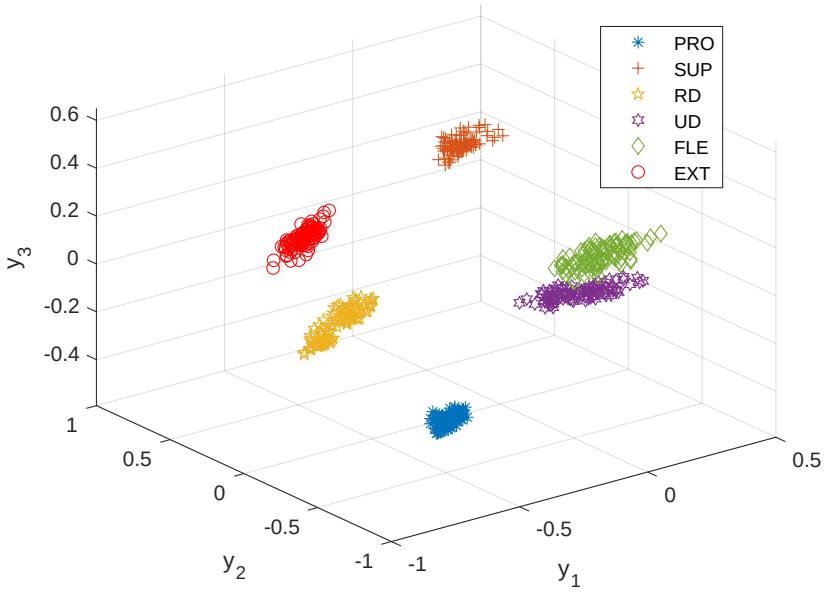

Figure 7: The output of joint activation of the BNN, where y_1, y_2, and y_3 are the axes for the DoFs for RD/UD, FLE/EXT and PRO/SUP, respectively.

although some boundaries are not very clear for the motions of FLE and EXT.

5. Conclusion and Future Works

This study presents an interpretable BNN model for wrist movement classification, which guarantees that the information propagation from sEMG signal to extremity is well modeled. The proposed model discloses the cooperative connection between active muscles and sEMG signals, as well as the internal relationship between hand gestures and muscles. The experiments show that the proposed model is able to decode wrist movements in an acceptable accuracy. More importantly, the model keeps interpretability after fine-tuning using the proposed ICBP algorithm, which is partly verified through the analysis of muscle activation and joint activation.

In the near future, finger movements will also be investigated to verify the success of the proposed model. Therefore, more muscles in the forearm will be

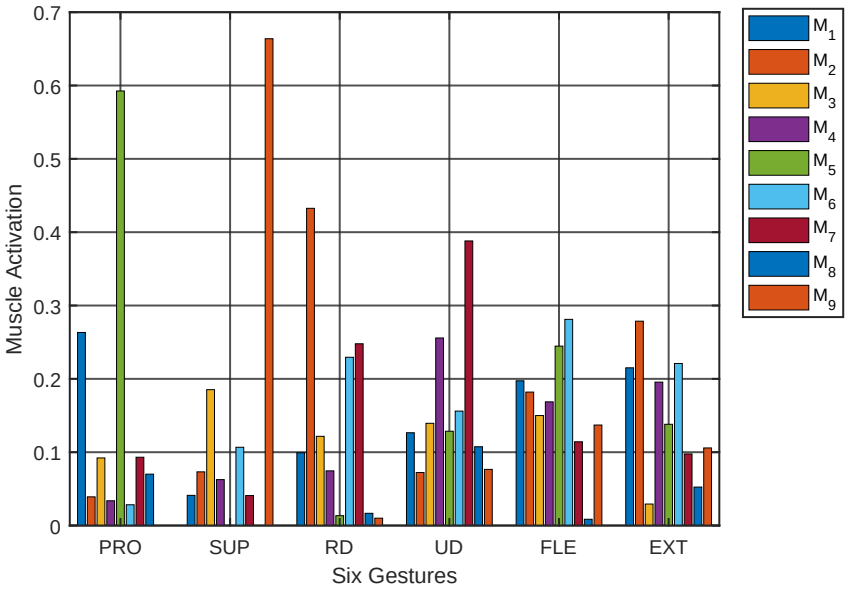

Figure 8: Averaged muscle activation across six subjects for nine investigated forearm muscles, when performing six wrist movements.

taken into account in the MA layer, and more DoFs will be included in the MS layer as well. Besides, the issues of electrode shift and cross subject variance will be investigated under the BNN model. Also, more comprehensive analysis on the parameters and the outputs of each layer will be conducted, expecting to explore the motion control mechanism of the central nervous system and understand the organization and coordination mechanisms of limb motion.

6. Acknowledgment

This work was supported in part by the basic public welfare research program of Zhejiang Province (No. LQ20F020016), the national natural science foundation of China (No. 52075530), the AiBle project co-financed by the European Regional Development Fund, the public funds of the State Key Laboratory of digital manufacturing equipment and technology of China (No. DMETKF2020027).

References

[1] D. Farina, N. Jiang, H. Rehbaum, A. Holobar, B. Graimann, H. Dietl, O. C. Aszmann, The extraction of neural information from the surface emg for the control of upper-limb prostheses: Emerging avenues and challenges, IEEE Transactions on Neural Systems & Rehabilitation Engineering 22 (4) (2014) 797–809.

[2] Z. Feng, P. Li, Z. G. Hou, L. Zhen, Y. Chen, Q. Li, T. Min, semg-based continuous estimation of joint angles of human legs by using bp neural network, Neurocomputing 78 (1) (2012) 139–148.

[3] X. Chen, D. Zhang, X. Zhu, Application of a self-enhancing classification method to electromyography pattern recognition for multifunctional prosthesis control, Journal of NeuroEngineering and Rehabilitation 10 (1) (2013) 44.

[4] C. Piazza, A. M. Simon, K. L. Turner, L. A. Miller, M. G. Catalano, A. Bicchi, L. J. Hargrove, Exploring augmented grasping capabilities in a multi-synergistic soft bionic hand, Journal of NeuroEngineering and Rehabilitation 17 (1) (2020) 1–16.

[5] C. Li, G. Li, G. Jiang, D. Chen, H. Liu, Surface emg data aggregation processing for intelligent prosthetic action recognition, Neural Computing and Applications 32 (22) (2020) 16795–16806.

[6] K. Kiguchi, T. Tanaka, T. Fukuda, Neuro-fuzzy control of a robotic exoskeleton with emg signals, IEEE Transactions on fuzzy systems 12 (4) (2004) 481–490.

[7] E. Repnik, U. Puh, N. Goljar, M. Munih, M. Mihelj, Using inertial measurement units and electromyography to quantify movement during action research arm test execution, Sensors 18 (9) (2018) 2767.

[8] D. Jiang, G. Li, Y. Sun, J. Kong, B. Tao, D. Chen, Grip strength forecast and rehabilitative guidance based on adaptive neural fuzzy inference system using semg, Personal and Ubiquitous Computing (2019) 1–10.

[9] J. J. A. Mendes Junior, M. L. B. Freitas, D. P. Campos, F. A. Farinelli, S. L. Stevan, S. F. Pichorim, Analysis of influence of segmentation, features, and classification in semg processing: A case study of recognition of brazilian sign language alphabet, Sensors 20 (16) (2020) 4359.

[10] S. Liu, C. Lin, Y. Chen, W. Chen, T. Huang, C. Hsu, An emg patch for the real-time monitoring of muscle-fatigue conditions during exercise, Sensors 19 (14) (2019) 3108.

[11] S. Guo, M. Pang, B. Gao, H. Hirata, H. Ishihara, Comparison of semg-based feature extraction and motion classification methods for upper-limb movement, Sensors 15 (4) (2015) 9022–9038.

[12] O. W. Samuel, H. Zhou, X. Li, H. Wang, H. Zhang, A. K. Sangaiah, G. Li, Pattern recognition of electromyography signals based on novel time domain features for amputees' limb motion classification, Computers & Electrical Engineering (2017) 646–655.

[13] B. Hudgins, P. Parker, R. N. Scott, A new strategy for multifunction myoelectric control, IEEE Transactions on Biomedical Engineering 40 (1) (1993) 82–94.

[14] Q. Ding, J. Han, X. Zhao, Y. Chen, Missing-data classification with the extended full-dimensional gaussian mixture model: Applications to emg-based motion recognition, IEEE Transactions on Industrial Electronics 62 (8) (2015) 4994–5005.

[15] Y. Fang, D. Zhou, K. Li, Z. Ju, H. Liu, Attribute-driven granular model for emg-based pinch and fingertip force grand recognition, IEEE transactions on cybernetics.

[16] D. Buongiorno, G. D. Cascarano, I. De Feudis, A. Brunetti, L. Carnimeo, G. Dimauro, V. Bevilacqua, Deep learning for processing electromyographic signals: A taxonomy-based survey, Neurocomputing 452 (2021) 549–565.

[17] Y. Cheng, G. Li, M. Yu, D. Jiang, J. Yun, Y. Liu, Y. Liu, D. Chen, Gesture recognition based on surface electromyography-feature image, Concurrency and Computation: Practice and Experience 33 (6) (2021) e6051.

[18] Z. Zhang, C. He, K. Yang, A novel surface electromyographic signal-based hand gesture prediction using a recurrent neural network, Sensors 20 (14) (2020) 3994.

[19] H. Chen, Y. Zhang, G. Li, Y. Fang, H. Liu, Surface electromyography feature extraction via convolutional neural network, International Journal of Machine Learning and Cybernetics 11 (1) (2020) 185–196.

[20] L. H. Gilpin, D. Bau, B. Z. Yuan, A. Bajwa, M. Specter, L. Kagal, Explaining explanations: An overview of interpretability of machine learning, in: 2018 IEEE 5th International Conference on Data Science and Advanced Analytics (DSAA), 2018.

[21] U. Côté-Allard, E. Campbell, A. Phinyomark, F. Laviolette, B. Gosselin, E. Scheme, Interpreting deep learning features for myoelectric control: A comparison with handcrafted features, Frontiers in bioengineering and biotechnology 8 (2020) 158.

[22] N. Jiang, K. B. Englehart, P. A. Parker, Extracting simultaneous and proportional neural control information for multiple-dof prostheses from the surface electromyographic signal, IEEE Transactions on Biomedical Engineering 56 (4) (2009) 1070–1080.

[23] C. M. Niu, Q. Luo, C.-h. Chou, J. Liu, M. Hao, N. Lan, Neuromorphic model of reflex for realtime human-like compliant control of prosthetic hand, Annals of Biomedical Engineering (2020) 1–16.

[24] X. Xi, Z. Sun, X. Hua, C. Yuan, Y.-B. Zhao, S. M. Miran, Z. Luo, Z. Lü, Construction and analysis of cortical–muscular functional network based on eeg-emg coherence using wavelet coherence, Neurocomputing 438 (2021) 248–258.

[25] D. Yang, J. Zhao, Y. Gu, L. Jiang, H. Liu, Emg pattern recognition and grasping force estimation: Improvement to the myocontrol of multi-dof prosthetic hands, in: IEEE/RSJ International Conference on Intelligent Robots and Systems, 2009.

[26] C. Meeker, S. Park, L. Bishop, J. Stein, M. Ciocarlie, Emg pattern classification to control a hand orthosis for functional grasp assistance after stroke, IEEE International Conference on Rehabilitation Robotics.

[27] D. Farina, I. Vujaklija, M. Sartori, T. Kapelner, F. Negro, N. Jiang, K. Bergmeister, A. Andalib, J. Principe, O. C. Aszmann, Man machine interface based on the discharge timings of spinal motor neurons after targeted muscle reinnervation, Nature biomedical engineering 1 (2) (2017) 1–12.

[28] G. Li, J. Li, Z. Ju, Y. Sun, J. Kong, A novel feature extraction method for machine learning based on surface electromyography from healthy brain, Neural Computing and Applications 31 (12) (2019) 9013–9022.

[29] I. Kyranou, S. Vijayakumar, M. S. Erden, Causes of performance degradation in non-invasive electromyographic pattern recognition in upper limb prostheses, Frontiers in neurorobotics 12 (2018) 58.

[30] S. Zhang, S. Guo, B. Gao, Q. Huang, M. Pang, H. Hirata, H. Ishihara, Muscle strength assessment system using semg-based force prediction method for wrist joint, Journal of Medical and Biological Engineering 36 (1) (2016) 121–131.

[31] T. Miller, Explanation in artificial intelligence: Insights from the social sciences, Artificial Intelligence 267 (2019) 1–38.

[32] D. J. Berger, A. d'Avella, Effective force control by muscle synergies, Frontiers in computational neuroscience 8 (2014) 46.

[33] A. Phinyomark, P. Phukpattaranont, C. Limsakul, Feature reduction and selection for emg signal classification, Expert systems with applications 39 (8) (2012) 7420–7431.

[34] J. Rafiee, M. Rafiee, F. Yavari, M. Schoen, Feature extraction of forearm emg signals for prosthetics, Expert Systems with Applications 38 (2011) 4058–4067.

[35] Y. Fang, X. Zhang, D. Zhou, H. Liu, Improve inter-day hand gesture recognition via convolutional neural network based feature fusion, International Journal of Humanoid Robotics.

[36] A. D. Bellingegni, E. Gruppioni, G. Colazzo, A. Davalli, R. Sacchetti, E. Guglielmelli, L. Zollo, Nlr, mlp, svm, and lda: a comparative analysis on emg data from people with transradial amputation, Journal of neuroengineering and rehabilitation 14 (1) (2017) 82.

[37] A. Waris, I. K. Niazi, M. Jamil, K. Englehart, W. Jensen, E. N. Kamavuako, Multiday evaluation of techniques for emg-based classification of hand motions, IEEE journal of biomedical and health informatics 23 (4) (2018) 1526–1534.